14th European Signal Processing Conference (EUSIPCO 2006), Florence, Italy, September 4-8, 2006, copyright by EURASIP

A FRAMEWORK FOR HISTOGRAM-INDUCED 3D DESCRIPTORS

Ceyhun Burak Akgül[1,3], Bülent Sankur[1], Yücel Yemez[2], and Francis Schmitt[3]

[1]Electrical and Electronics Engineering Dept., Boğaziçi University, Bebek, Istanbul, Turkey
[2]Computer Engineering Dept., Koç University, Rumelifeneri, Istanbul, Turkey
[3]Dept. Signal-Image, Ecole Nationale Supérieure des Télécommunications, Paris, France
ceyhun.akgul@boun.edu.tr, bulent.sankur@boun.edu.tr, yemez@ku.edu.tr, francis.schmitt@enst.fr

ABSTRACT

We present a novel framework to describe 3D shapes, based on modeling the probability density of their shape functions. These functions are conceived to reflect the 3D geometrical properties of the shape surfaces. The densities are modeled as mixtures of Gaussians, each component being the distribution induced by a mesh triangle. A fast algorithm is developed exploiting both the special geometry of 3D triangles with numerical approximations as well as a transform technique. We test and compare the proposed descriptors to other histogram-based methods on two different 3D model databases. It is shown that 3D shape descriptors outperform all of its competitors except one in retrieval applications. Furthermore our methodology provides a fertile ground to introduce and test new descriptors.

1. INTRODUCTION

The use of 3D models is becoming increasingly more commonplace in many fields of computer graphics, such as computer-aided design, medical imaging, molecular analysis or presentation of cultural heritage in a virtual environment. The organization and access to 3D shape databases demands effective tools for indexing, retrieval, categorization, classification and representation of shapes. These operations necessitate shape matching, that is, determining the distance between two shapes or the extent to which two shapes resemble each other [8]. Representations used for shape matching are often referred to as *3D shape descriptors* encoding geometrical and topological properties of an object in a discriminative and compact manner. Reference [8] reflects the diversity of 3D shape descriptors proposed in the literature.

In this work, we focus exclusively on histogram-based 3D shape descriptors [2-5, 11]. Our interest in histogram-based 3D shape descriptors stems from the fact that they are global descriptors by nature and they are instrumental in classifying shapes into broad categories [8]. Previous approaches in the literature have computed a generic histogram-based descriptor by first computing geometrical quantities, called *shape functions*, using the surface points of a 3D triangular mesh, and then by accumulating the scores into histogram bins. In contrast to their empirical approach, we follow a more analytical method. Our framework, in fact, relies on imposing a density model for each triangle in the mesh. That is, we estimate the density of the shape function for each triangle individually and calculate the overall density as a mixture of mesh face induced densities.

In histogram-based 3D shape descriptors, the surface points are either chosen as the centers of gravity of the triangles or are obtained by randomly and profusely sampling points from the surface. The former approach suffers from the fact the triangles making up the mesh may have arbitrary forms and sizes; hence the triangle centers may not be sufficiently representative. The random sampling of the surface may compensate for the non-uniformity of the form and size of the triangles, provided that a sufficiently large number of surface points is taken. For multivariate shape functions, however, the accurate estimation of joint histograms can suffer from the curse of dimensionality [1]. Our modeling framework takes care of the non-uniform distribution of triangles without resorting to random sampling. We model the density of shape functions in terms of simpler distributions. We have chosen the Gaussian density, not only due to its maximum entropy interpretation in terms of moments, but also because we can make use of the fast algorithm to compute mixture density. Since the Gaussian density is completely determined by its first two moments, we need only to estimate the mean and the variance of the shape function for each triangle. For certain cases, these moments can be approximated very accurately by making use of the geometry of the 3D triangles. Thus the shape descriptors are obtained as large mixtures of Gaussians. Despite the reduction of the shape function density to the estimation of its Gaussian moments, the computation can still be heavy. This computational burden is alleviated by the use of an efficient algorithm: the *Fast Gauss Transform* (FGT) [10] to calculate expressions involving large sums of Gaussians.

The main contribution of our work is an analytical framework for 3D descriptors extracted from shape functions that characterize object geometry. Our approach has the advantage of being computationally efficient and more accurate compared to other histogram methods. As a byproduct, we also introduce some novel shape functions.

The next section describes our computational framework. In Section 3, we illustrate the performance of our method in comparison to other equivalent or similar histogram-based descriptors [2-5, 11] in a retrieval application on two different 3D model databases. In Section 4, we draw conclusions and discuss further directions in histogram-based 3D shape descriptors.

2. METHOD

We assume that each 3D shape is represented with a triangular mesh and that its center of mass coincides with the origin of the coordinate system. Hence all descriptors are translation invariant. In what follows, capital italic letter P stands for a point in 3D, a small case boldface letter $\mathbf{p}=(p_x,p_y,p_z)$ for its vector representation, $\mathbf{n}_P=(n_{P,x},n_{P,y},n_{P,z})$ for the unit surface normal vector at P when P belongs to a surface $M\subset\mathbb{R}^3$ and $\cdot$ for the usual dot product.

2.1 Shape functions

A multidimensional shape function S of a surface $\mathcal{M}\subset\mathbb{R}^3$ is a mapping from the points of this surface into a d-dimensional space, generally $\mathbb{R}^d$. Each dimension of this space corresponds to a specific geometric measure, which can be calculated at each point of the surface. For example, the distance of a surface point to the barycenter of the 3D shape is a one-dimensional (d = 1) shape function. We consider three classes of shape functions:

- The *radial* shape function S_r is defined as $S_r(\mathbf{p})=\sqrt{\mathbf{p}\cdot\mathbf{p}}$, $P\in\mathcal{M}$. This rotation-invariant shape function corresponds to the distance of a surface point to the center of mass of the shape, and is equivalent to Pacquet et al.'s "cord" length [5] and Osada et al.'s D1-shape function [4]. The distribution of the radial shape function indicates the extent to which the surface of the shape deviates from a perfect sphere, the distribution of a sphere being a delta-Dirac distribution.
- The *surface angles*, which can be written in generic form as $S_{a,\mathbf{v}}(\mathbf{p})=\mathbf{p}\cdot\mathbf{v}/\sqrt{\mathbf{p}\cdot\mathbf{p}}$ where $\mathbf{v}$ is some unit norm vector. One instance of this function is obtained by letting $\mathbf{v}$ be the surface normal vector $\mathbf{n}_P$ at P. In this case, the shape function is scale and rotation invariant. If the local surface approximates a spherical cap then the vectors $\mathbf{p}$ and $\mathbf{n}_P$ align, and $S_{a,\mathbf{v}}$ approaches unity. An alternative $S_{a,\mathbf{v}}$-shape function reflecting also some global property of the surface is given by associating $\mathbf{v}$ with one or more of the eigen-directions $\{\mathbf{q}_1,\mathbf{q}_2,\mathbf{q}_3\}$ of the mesh, based on the eigen-decompositon of the covariance matrix [8]. Pacquet et al. consider the largest two of these directions $\{\mathbf{q}_1,\mathbf{q}_2\}$ [5].
- The *tangent plane* shape function S_t of a surface point is a parameterization of the local tangent plane at point P in terms of spherical coordinates. Specifically, S_t is a three-dimensional shape function $S_t=(s,\theta,\varphi)$ where $s=|\mathbf{p}\cdot\mathbf{n}_P|$, $\theta=\tan^{-1}(n_{P,y}/n_{P,x})$, $\varphi=\cos^{-1}(n_{P,z})$ with $\theta\in[0,2\pi]$, $\varphi\in[0,\pi]$. The density of this shape function is akin to the 3D Hough transform descriptor [11].

Except for S_t, all of the shape functions presented so far are one-dimensional. However, it is possible to combine these single-valued functions to obtain multi-valued functions that capture the shape information in a better way.

2.2 Probability density evaluation

We first calculate analytically the shape function density of an arbitrary surface triangle T_k, and then obtain the density for the whole mesh $\mathcal{M}$ as a mixture of individual densities, since the mesh itself is the union of K triangles. The probability density function $f(S)$ of a shape function S (where S is a random variable or a random vector) is defined over $\mathcal{M}$. Consider a general d-dimensional shape function, i.e., $S(\mathbf{p})=(S_1(\mathbf{p}),...,S_d(\mathbf{p}))$. Since the mesh triangles are disjoint except for neighboring edges, we may write

$$f(S)=\sum_{k=1}^{K} f(S,P\in T_k). \tag{1}$$

The summand in (1) can be expressed as the joint density of S and a binary indicator variable, which is one if $P\in T_k$, and zero otherwise. Conditional to this variable, the joint density can be written as $f(S,P\in T_k)=f(S|P\in T_k)\Pr(P\in T_k)$, where $\Pr(P\in T_k)$ is the probability of a surface point P to belong to the triangle T_k. This is simply the ratio w_k of the area of T_k to the total surface area. Eq. (1) becomes

$$f(S)=\sum_{k=1}^{K} w_k f(S|P\in T_k)=\sum_{k=1}^{K} w_k f_k(S), \tag{2}$$

where $f_k(S)$ is the density of S when P is restricted to lie inside the triangle T_k. Thus, the remaining task reduces to evaluating the density of a shape function for individual triangles in 3D space. To evaluate the conditional density $f_k(S)$, we assume Gaussian density models for all shape functions. For a d-dimensional shape function S over the triangle T_k, we then rewrite $f_k(S)$ as

$$f_k(S)=(2\pi)^{-d/2}|\Sigma_k|^{-1/2}\exp\left(-\frac{1}{2}(S-\mu_k)^t\,\Sigma_k^{-1}(S-\mu_k)\right), \tag{3}$$

where μ_k is the d-dimensional mean vector and Σ_k is the covariance matrix. Thus, in the general case, we only need μ_k and Σ_k to fully specify the density.

Case 1: <u>One-dimensional shape function</u>

Let T be an arbitrary triangle in 3D space with vertices A, B, and C represented by $\mathbf{p}_A,\mathbf{p}_B$, and $\mathbf{p}_C$ respectively. By noting $\mathbf{e}_1=\mathbf{p}_B-\mathbf{p}_A$ and $\mathbf{e}_2=\mathbf{p}_C-\mathbf{p}_A$, we have the following parametric representation of an arbitrary point P inside the triangle T as $\mathbf{p}=\mathbf{p}_A+x\mathbf{e}_1+y\mathbf{e}_2$, where the two parameters x and y satisfy the constraints: $x,y\geq 0$ and $x+y\leq 1$. We also assume that points $\{P\}$ are uniformly distributed inside the triangle T. Thus, the estimation of $f_k(S)$ reduces to the

estimation of the first and second order moments of $S(x,y)$. The n^{th} order moment of $S(x,y)$ can be evaluated as

$$E\{S^n\} = \iint_{\substack{x,y\geq 0 \\ x+y\leq 1}} S^n(x,y) f(x,y)\,dxdy\,, \qquad (4)$$

where $f(x,y)$ is the uniform density of the pair (x,y) within the domain $x,y \geq 0$ and $x+y \leq 1$. For the second order moment of the radial shape function S_r, we have an analytical expression: $E\{S_r^2\} = (1/6)(a+b+c)+(2/3)(d+e)+h$, where $a = \mathbf{e}_1 \cdot \mathbf{e}_1$, $b = \mathbf{e}_2 \cdot \mathbf{e}_2$, $c = \mathbf{e}_1 \cdot \mathbf{e}_2$, $d = \mathbf{p}_A \cdot \mathbf{e}_1$, $e = \mathbf{p}_A \cdot \mathbf{e}_2$, and $h = \mathbf{p}_A \cdot \mathbf{p}_A$. However, for other functions and/or moment orders we have to resort to numerical integration. A double application of Simpson's 1/3 rule [6] at the midpoints of the integration intervals in (4) gives

$$E\{S^n\} \approx \frac{1}{18}\{S^n(0,0) + 4S^n(0,1/2) + S^n(0,1) + 2S^n(1/2,0) + 8S^n(1/2,1/4) + 2S^n(1/2,1/2)\}\,. \qquad (5)$$

Notice that this estimate boils down to a weighted sum $S^n(x,y)$ evaluated at 6 points on the borders of the triangles. To illustrate the viability of this approximation, we have generated 1000 triangles in 3D space with arbitrary sizes and shapes by uniform random vectors $\mathbf{p}_A, \mathbf{e}_1$, and $\mathbf{e}_2$ and analyzed the error of our approximation scheme for the first-order moment of the S_r-shape function. The first estimate $\hat{S}_r^{\text{MC}}$ was obtained by a Monte Carlo (MC) approach, with one million samples per triangle. $\hat{S}_r^{\text{MC}}$ being a very accurate estimate of the true mean of the S_r-shape function, we considered it as the ground truth. The second and third estimates $\hat{S}_r^{\text{Center}}$ and $\hat{S}_r^{\text{Simpson}}$ were calculated respectively, by sampling each triangle at its center of gravity and by using Equation (5). The ratio (averaged over 1000 triangles) between the absolute error $\left|\hat{S}_r^{\text{Center}} - \hat{S}_r^{\text{MC}}\right|$ of the centroidal approximation and that of our estimate $\left|\hat{S}_r^{\text{Simpson}} - \hat{S}_r^{\text{MC}}\right|$ was 82, indicating the superior accuracy of the approximation using (5) over the centroidal approximation. Therefore, we use the numerical scheme given in (5) to evaluate the mean $\mu = E\{S\}$ and the variance $\sigma^2 = \left(E\{S^2\} - E\{S\}^2\right)$ of any given shape function *S* for any given triangle *T*.

Case 2: Multidimensional shape function

In contrast to the one-dimensional case, the computation of large sums of Gaussians might be prohibitive in higher dimensions [10]. For multidimensional shape functions, in order to keep the complexity of the method at a tractable level, we have used the FGT algorithm, which provides significant speedups compared to direct evaluation [10]. However, the FGT implementation that we have does not allow us to specify a distinct full covariance matrix for each triangle. In order to make use of FGT, we set a fixed covariance matrix for all triangles, $\Sigma = \Sigma_1 = ... = \Sigma_K$, where Σ is a diagonal matrix, i.e., $\Sigma = diag\left(\sigma_1^2, ..., \sigma_d^2\right)$. The discarded off-diagonal terms have been experimentally observed to be insignificant. Notice that the *d* shape function components will still be assigned different variances, but these variances are assumed to be identical in all the triangles. After these simplifications, in the multidimensional case, $f(S)$ becomes

$$f(S) = (2\pi)^{-d/2}\left(\sigma_1 ... \sigma_d\right)^{-1} \sum_{k=1}^{K} w_k \exp\left(-\frac{1}{2}\sum_{i=1}^{d}\left(\frac{S_i - \mu_{k,i}}{\sigma_i}\right)^2\right). \qquad (6)$$

This suggests that, for multidimensional shape functions, the choice of the global covariance, much like in a Parzen-window approach [1], can be done in application and/or database-dependent manner. In other words, we have optimized these parameters by a search technique for the best discriminative performance for specific goals such as categorization or content-based retrieval. This global approach becomes, in fact, a necessity in the case of the multidimensional shape function S_t. Recall that this shape function involves the spherical parameterization of the tangent plane of a surface point. For a triangular mesh, the tangent plane of a surface point *P* is identical with the plane carrying the triangle to which *P* belongs. Therefore for all surface samples in that triangle S_t would be identical, leading to zero variance for all components. However, we can still use Gaussian modeling but with global variance as explained in the previous paragraph.

3. EXPERIMENTS

In this section, we illustrate the performance of the framework described above in a 3D model retrieval application. In a typical retrieval system, descriptors of all objects in the database are stored. When a query model is presented to the system, its descriptor is calculated and then compared to all of the stored descriptors using a distance function. Finally, database models are sorted in terms of increasing distance values. The models on the top of the resulting list are expected to resemble the queried model more than those on the bottom of the list. We have experimented on two 3D model databases: the Princeton Shape Benchmark (PSB) [7] and the Sculpteur Database (SCUdb) [9]. Both databases consist of objects described as triangular meshes, though they differ substantially in terms of content and mesh quality. PSB is a publicly available database containing a total of 1814 models, categorized into general classes such as animals, humans, plants, tools, vehicles, buildings, etc. An important feature of the database is the availability of two equally sized sets: Training (90 classes) and Test (92 classes). On the other hand, SCUdb is a private database containing over 800 models corresponding to mostly archeological objects residing in museums [9]. Presently, 513 of the models are classi-

fied into 53 categories including utensils of ancient times, pavements, and various artistic objects. The meshes in SCUdb are highly detailed and reliable in terms of connectivity and orientation of triangles.

Next, we present the retrieval results in terms of precision-recall curves, nearest neighbor (**NN**) and discounted cumulative gain (**DCG**) values [7]. Precision and recall are generally presented together as a precision-recall curve, which should be ideally a horizontal line at unit precision. NN stands for the percentage of the closest matches that belong to the same class as the query. DCG is a statistic that weights correct results near the front of the list more than correct results later in the ranked list. Normalized discounted cumulative gain (**NDCG**) is based on averaging DCG values of a set of algorithms on a database. A negative NDCG value means that the performance of the algorithm is below the average; similarly a positive value indicates an above average performance [7].

We have implemented and tested the following histogram-based descriptors proposed in the literature [5, 4, 2, 3, 11, respectively] with their specified descriptor size N:

- **[Cord, A1, A2]**: Cord and angle histograms, $N = 64\times3$,
- **[D1,D2]**: D1 and D2 distributions concatenated, $N = 64\times2$,
- **EGI**: Extended Gaussian image, $N = 8^2 = 64$,
- **CEGI**: Complex extended Gaussian image, $N = 8^2 = 64$,
- **3DHT**: 3D Hough Transform Descriptor, $N = 8^3 = 512$.

The descriptors developed in the present work and compared to those given above are:

- **[S1,S2]**: $S_r, S_{a,\mathbf{n}_P}$ -densities concatenated, $N = 64\times2$,
- **[S1,S3,S4]**: $S_r, S_{a,\mathbf{q}_1}, S_{a,\mathbf{q}_2}$ -densities concatenated, $N=64\times3$,
- **[S1,S2,S3,S4]**: S_r, $S_{a,\mathbf{n}_P}$, $S_{a,\mathbf{q}_1}$, $S_{a,\mathbf{q}_2}$ -densities concatenated, $N = 64\times4$,
- **(S1,S2)**: $(S_r, S_{a,\mathbf{n}_P})$ -joint density, $N = 8^2 = 64$,
- **(S1,S3,S4)**: $(S_r, S_{a,\mathbf{q}_1}, S_{a,\mathbf{q}_2})$ -joint density, $N = 8^3 = 512$,
- **(S1,S2,S3,S4)**: $(S_r, S_{a,\mathbf{n}_P}, S_{a,\mathbf{q}_1}, S_{a,\mathbf{q}_2})$ -joint density, $N = 8^4 = 4096$,
- **St**: S_t -density, $N = 8^3 = 512$.

Note that concatenated densities refers to the juxtaposition of two or more univariate densities; on the other hand, joint-density refers to a genuine multivariate density. The binning procedure is as follows: we quantize the range of each component into 8 uniform bins in both the univariate or multivariate cases. This gives a descriptor of size 8^d for a d-dimensional shape function. For descriptors that are not scale invariant, we rescale the models so that the area weighted average distance of surface points to the center of mass is unity. We have observed that distance components of normalized shapes exceeds 2 with a very low probability, hence we have fixed their upper limit to 2. Finally, for descriptors that are not rotation-invariant, we realigned the models with their principal directions. The retrieval statistics are tabulated in

Table 1 Retrieval Statistics for Histogram-based Descriptors for PSB Training Set (Positive NDCGs are shown in gray)

Descriptor	NN	DCG	NDCG
[Cord, A1, A2]	0.280	0.398	-0.175
[D1, D2]	0.356	0.446	-0.075
[S1, S2]	0.363	0.462	-0.043
[S1, S3, S4]	0.395	0.471	-0.023
[S1, S2, S3, S4]	0.451	0.506	0.049
(S1, S2)	0.448	0.496	0.029
(S1, S3, S4)	0.427	0.470	-0.026
(S1, S2, S3, S4)	0.508	0.508	0.053
EGI	0.366	0.445	-0.078
CEGI	0.436	0.477	-0.011
3DHT	0.592	0.563	0.168
St	0.556	0.545	0.130

Table 2 Retrieval Statistics for Histogram-based Descriptors for PSB Test Set (Positive NDCGs are shown in gray)

Descriptor	NN	DCG	NDCG
[Cord, A1, A2]	0.249	0.394	-0.156
[D1, D2]	0.323	0.434	-0.071
[S1, S2]	0.324	0.440	-0.057
[S1, S3, S4]	0.380	0.456	-0.022
[S1, S2, S3, S4]	0.440	0.492	0.055
(S1, S2)	0.412	0.474	0.016
(S1, S3, S4)	0.397	0.447	-0.044
(S1, S2, S3, S4)	0.470	0.484	0.037
EGI	0.315	0.436	-0.066
CEGI	0.375	0.463	-0.008
3DHT	0.578	0.556	0.191
St	0.508	0.526	0.126

Table 3 Retrieval Statistics for Histogram-based Descriptors for SCUdb (Positive NDCGs are shown in gray)

Descriptor	NN	DCG	NDCG
[Cord, A1, A2]	0.604	0.623	-0.087
[D1, D2]	0.665	0.660	-0.032
[S1, S2]	0.692	0.686	0.006
[S1, S3, S4]	0.643	0.642	-0.059
[S1, S2, S3, S4]	0.715	0.693	0.017
(S1, S2)	0.727	0.729	0.069
(S1, S3, S4)	0.628	0.619	-0.092
(S1, S2, S3, S4)	0.715	0.672	-0.015
EGI	0.630	0.644	-0.056
CEGI	0.694	0.703	0.031
3DHT	0.778	0.772	0.132
St	0.749	0.740	0.086

Tables 1-3. Precision-recall curves are displayed in Figures 1-3. On these retrieval results, we can provide the following comments:

- In all cases, our combined descriptors proved to be superior to [Cord, A1, A2] and [D1, D2]. The only exception is that for SCUdb, [D1, D2] is better than our [S1, S3, S4] descriptor. While the joint density descriptor (S1, S2) has significantly improved its concatenated version [S1, S2], the other joint density descriptors yield performances similar to their concatenated versions. The St descriptor has the best performance among all our proposed joint descriptors, and it is second only to 3DHT. More than half of our descriptors have positive NDCG, beating EGI and CEGI.
- The two best descriptors, 3DHT and St, are based on tangent plane, indicating that tangent plane can capture the shape information better than other geometric measures.

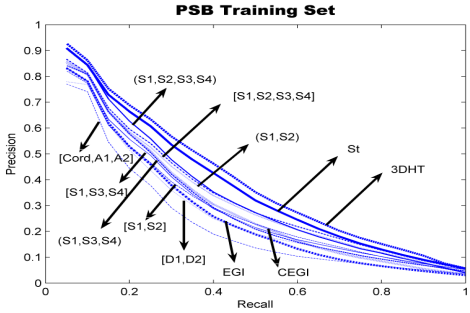

Figure 1 Precision-recall curves for histogram-based 3D shape descriptors on PSB Training Set

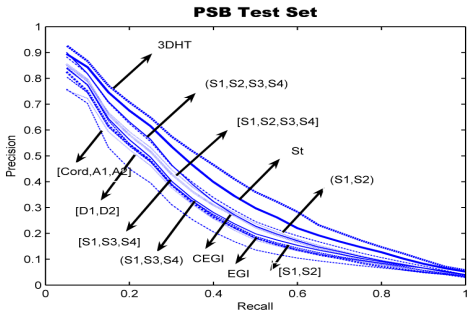

Figure 2 Precision-recall curves for histogram-based 3D shape descriptors on PSB Test Set

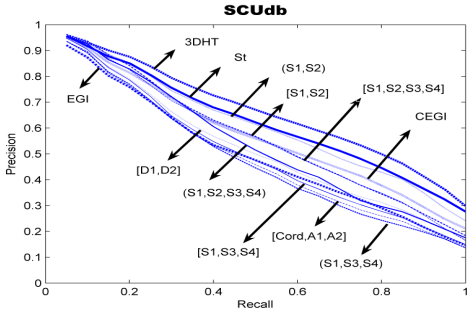

Figure 3 Precision-recall curves for histogram-based 3D shape descriptors on SCUdb

- NN performances of our descriptors prove to be better than other histogram-based descriptors except 3DHT, indicating their potential in recognition applications.

4. DISCUSSION AND CONCLUSION

We have proposed a framework to compute histogram-based 3D shape descriptors and evaluated its impact in a retrieval scenario. We have shown that shape descriptors, derived as Gaussian mixtures, prove more advantageous compared to the count-and-accumulate based histogram descriptors. First, it is computationally feasible as compared to Monte Carlo sampling; second, its performance is superior as to when histograms were estimated with a single sample per triangle. Third, most importantly, our framework is robust against mesh resolution and it can cope with mesh triangles of arbitrary shapes and sizes. In fact, our framework can be viewed as an application of kernel density estimation [1].

The use of probability density models other than Gaussians is conceivable. The choice of Gaussian model is motivated by its maximum entropy interpretation whenever only the first two moments (mean and variance estimates) are available. Especially for multidimensional shape functions, Gaussian model provides a more gracious control over finite sample-size problems, while the control in multivariate histograms is limited to bin width adjustments [1]. The variance parameter of Gaussians can be optimized in a database-dependent manner.

In summary, a general framework for shape distribution-based approaches has been developed, that covers under its umbrella existing and novel descriptors. Our method enables the use of arbitrary (possibly multidimensional) shape functions for retrieval, recognition, and classification of 3D objects. An immediate problem is to evaluate their performance in a recognition application, a clue being the favorable NN scores of our descriptors. Other future research will concentrate on investigating probability models that preserve neighborhood information, exploitation of multi-scale information, and information-theoretic limits of our approach.

5. ACKNOWLEDGEMENTS

This research was supported by BU Research Fund 03A203 and TUBITAK Project 103E038.

REFERENCES

[1] R. O. Duda, P. E. Hart, and D. G. Stork, *Pattern Classification*, 2nd edition, Wiley Interscience, 2000.

[2] B. Horn, "Extended gaussian image", *Proc. of the IEEE*, vol. 72, pp. 1671-1686, 1984.

[3] S. B. Kang and K. Ikeuchi, "The complex EGI: a new representation for 3d pose determination, *IEEE Trans. on PAMI*, vol. 16, pp. 249-258, 1994.

[4] R. Osada, T. Funkhouser, B. Chazelle, and D. Dobkin, "Shape distributions", *ACM Trans. on Graphics*, vol. 21, pp. 807-832, 2002.

[5] E. Paquet and M. Rioux, "Nefertiti: a query by content software for three-dimensional models databases management", *Image and Vision Computing*, vol. 17, pp. 157-166, 1999.

[6] W. H. Press, B. P. Flannery, and S. A. Teukolsky, *Numerical Recipes in C*, Cambridge University Press, 1992.

[7] P. Shilane, P. Min, M. Kazhdan, and T. Funkhouser, "The Princeton Shape Benchmark", *in Proc. Shape Modeling International (SMI'04)*, Italy, 2004, pp. 167-178.

[8] J. W. Tangelder and R. C. Veltkamp, "A survey of content based 3d shape retrieval methods", *in Proc. Shape Modeling International (SMI'04)*, Italy, 2004, pp. 145-156.

[9] T. Tung and F. Schmitt, "The augmented multiresolution Reeb graph approach for content-based retrieval of 3D shapes, *International Journal of Shape Modeling*, vol.11, pp. 91-120, 2005.

[10] C. Yang, R. Duraiswami, N. A. Gumerov, and L. Davis, "Improved Fast Gauss Transform and Efficient Kernel Density Estimation", *in Proc. Int. Conf. Computer Vision*, Nice, France, 2003, pp. 464-471.

[11] T. Zaharia and F. Prêteux, "Indexation de maillages 3d par descripteurs de forme", *in Proc. Reconnaissance des Formes et Intelligence Artificielle (RFIA'02)*, Angers, France, 2002, pp. 48-57.